Accelerated Lifetime Testing of High Power Lithium Titanate Oxide Batteries

Stroe, Ana-Irina; Stroe, Daniel-Ioan; Knap, Vaclav; Maciej, Swierczynski; Teodorescu, Remus

Published in:
Proceedings of the 2018 IEEE Energy Conversion Congress and Exposition (ECCE)

DOI (link to publication from Publisher):
10.1109/ECCE.2018.8557416

Publication date:
2018

Document Version
Accepted author manuscript, peer reviewed version

Accelerated Lifetime Testing of High Power Lithium Titanate Oxide Batteries

Ana-Irina Stroe
Department of Technology
Aalborg University
Aalborg, Denmark
ast@et.aau.dk

Daniel-Ioan Stroe
Department of Technology
Aalborg University
Aalborg, Denmark
dis@et.aau.dk

Vaclav Knap
Department of Technology
Aalborg University
Aalborg, Denmark
vkn@et.aau.dk

Maciej Swierczynski
Lithium Balance A/S
Smørum, Denmark
mas@lithiumbalance.com

Remus Teodorescu
Department of Technology
Aalborg University
Aalborg, Denmark
ret@et.aau.dk

***Abstract*—This paper presents results obtained from extensive accelerated lifetime tests performed on a high power Lithium Titanate Oxide (LTO) battery cell. The tests were performed at elevated temperatures, with different C-rates, and for different cycle depths. The obtained results have shown a very good capacity retention and a reduced internal resistance increase (and subsequently reduced power capability decrease) even after more than 8000 cycles performed at 42.5°C. We found out that both the capacity and the internal resistance have been degrading faster when the LTO-based battery cells were cycled with a smaller C-rate (i.e., 1C) than with a higher C-rate (i.e., 3C). Moreover, based on the harvested aging results, we discovered that the capacity and not the internal resistance is the performance parameter of the tested LTO-based battery cells, which will limit their lifetime.**

Keywords—Lithium-Ion Battery, Lithium Titanate Oxide, Accelerated Aging, Capacity Fade, Resistance Increase

I. INTRODUCTION

Since their market introduction in the 1990s, Lithium-ion (Li-ion) batteries have gradually become the key energy storage technology for various applications. Nowadays, Li-ion batteries represent the most suitable battery technology for powering electric vehicles [1], [2]. Furthermore, Li-ion batteries energy storage systems are used in various renewable energy storage applications, such as grid frequency regulation [3], renewables' grid integration [4] etc. This has become possible because Li-ion batteries are characterized by high gravimetric and volumetric energy density, high efficiency, high power capability during both charging and discharging, and long lifetime [5].

As discussed in [6], different Li-ion battery chemistries are available to the users. The vast majority of these chemistries are based on a graphite carbon anode and a lithium metal oxide (e.g., NMC, NCA etc.) cathode. However, these chemistries still raise different questions to the OEMs in terms of safety, cycle stability and performance at low and high temperature [2]. Thus, new electrode materials have been developed for Li-ion batteries in the past years. This is the case of the Lithium Titanate Oxide – $Li_4Ti_5O_{12}$ (LTO), which represents a very appealing anode material [7]. Even though characterized by lower energy density and lower nominal voltage (i.e., 2.2-2.3 V) than traditional graphite-based Li-ion batteries, the LTO-based batteries have several advantages such as: increased safety, high cycling stability, high rate charge-discharge capability even at low temperatures, long lifetime, and no solid electrolyte interface formation [2], [8].

Different aspects regarding LTO-based batteries have been studied and are available in the literature. Most of these are related to their electrochemical performance improvement [9], [10] while others are related to the understanding of their performance behavior [2], [11]. Nevertheless, there are very few studies, which focused on analyzing the degradation and lifetime behavior of the LTO-based battery chemistry.

Therefore, in this paper, we evaluate the degradation behavior of a commercially available high power LTO-based battery cell by analyzing the results obtained from extensive aging tests. As LTO-based batteries are characterized by very long lifetime, they were subjected to an accelerated aging procedure, similar to the methodologies presented in [12] and [13].

II. EXPERIMENT SET-UP

A. LTO-based Battery Cell

In this work, high power pouch-format Li-ion battery cells with a nominal voltage of 2.26 V and a nominal capacity of 13 Ah were used; LTO and NMC are used as active materials for the anode and cathode, respectively. The main electro-thermal parameters of the tested LTO-based battery cell are summarized in Table I.

TABLE I. MAIN PERFORMANCE PARAMETERS OF THE TESTED LTO-BASED BATTERY CELLS

Performance Parameter	Values
Nominal Capacity	13 Ah
Nominal Voltage	2.26 V
Discharge Cut-off Voltage	1.5 V (from -40 ºC to +30 ºC) 1.8 V (from +30 ºC to +55 ºC)
Charge Cut-off Voltage	2.8 V (from -40 ºC to +30 ºC) 2.9 V (from +30 ºC to +55 ºC)
Max. Continuous Charge/ Discharge Current	130 A (10 C-rate)
Pulse Charge/ Discharge Current (10 s)	260 A
Cycling and Storage Temperature	-40 ºC to +55 ºC

B. *Accelerated Cycle Lifetime Testing*

The LTO-based battery cells were subjected to extensive accelerated cycle lifetime tests at the conditions summarized in Table II. For all the cycle aging conditions presented in Table 2, an average SOC level of 50% was considered. Furthermore, the mentioned temperatures are the ones measured in the middle of the cell using a K-type 100 thermocouple. Two LTO-based cells have been tested under the same conditions in order to eliminate any possible outliers and for statistical relevance.

The number of full equivalent cycles (FEC) to which the battery cells have been subjected at each individual condition is also presented in Table 2. The tests, which had been performed at conditions TC2 and TC3, were stopped after 3500 and 4500 FEC, respectively, as the battery achieved a very high degradation (as it will be shown in the next section).

C. *Reference Performance Test Procedure*

In order to quantify the gradual degradation of the performance parameters of the tested LTO-based battery cells, the so-called reference performance tests (RPT) were performed regularly. In the beginning, RPTs were performed after each 100 FEC (i.e., when 2600 Ah went through the battery); however, due to a very slow degradation of the batteries, which had been initially observed, it was decided to perform the following RPTs with a resolution of 200 FEC (i.e., 5200 Ah throughput).

The RPTs were composed of a capacity test, internal resistance measurements, and electrochemical impedance spectroscopy (EIS) measurements. The battery capacity was determined for a current of 13 A (i.e., 1C-rate) for both charging and discharging regimes. The internal resistance of the battery was measured using the DC pulse technique at various state of charge (SOC) levels using the current train pulse profile illustrated in Fig. 1, which was extenisvely described in [14]. The small-signal AC impedance of the battery was measured using the EIS technique following the same procedure as for the internal resistance measurements. All the RPTs were performed at 25ºC. An example of the current, voltage and temperature profiles, measured during one RPT is presented in Fig. 2.

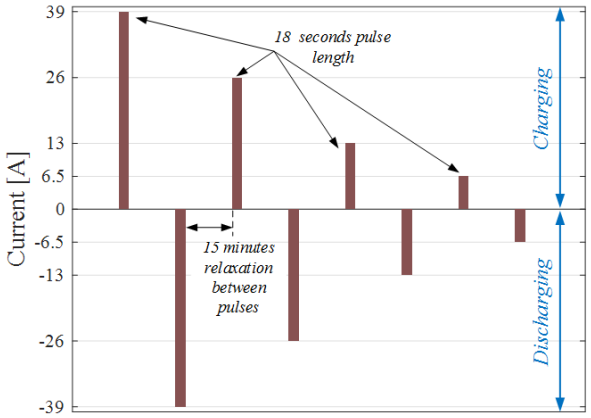

Fig. 1. Current train pulse profile for measuring the internal resistance of the LTO-based battery cells.

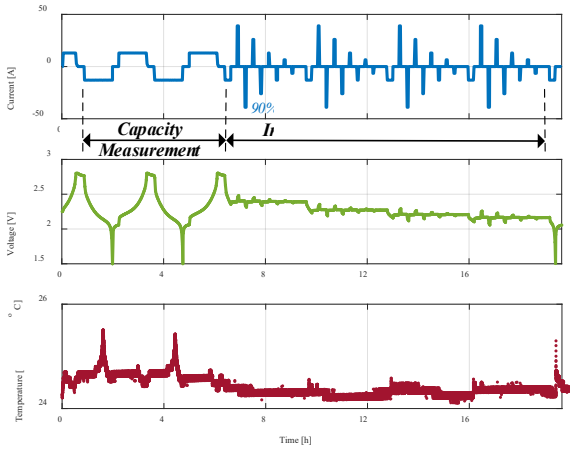

Fig. 2. Current (top), voltage (middle), and temperature (bottom) signals during one RPT.

TABLE II. ACCELERATED AGING CONDITIONS AND THE CORRESPONDING NUMBER OF CYCLES TO WHICH THE LTO-BASED BATTERY CELLS WERE SUBJECTED

Test Case	Aging Conditions			Number of Cycles Performed
	Temperature	*Cycle Depth*	*Charging/ Discharging Current*	
TEST CASE 1	50 ºC	10 %	2C / 2C	6200 FEC[a]
TEST CASE 2	50 ºC	50 %	1C / 1C	3500 FEC
TEST CASE 3	50 ºC	50 %	2C / 2C	4500 FEC
TEST CASE 4	42.5 ºC	10 %	2C / 2C	7400 FEC
TEST CASE 5	42.5 ºC	30 %	2C / 2C	7000 FEC
TEST CASE 6	42.5 ºC	50 %	1C / 1C	4100 FEC
TEST CASE 7	42.5 ºC	50 %	2C / 2C	6000 FEC
TEST CASE 8	42.5 ºC	50 %	3C / 3C	8700 FEC

[a] FEC denotes one full equivalent cycle

III. Aging Results

A. Capacity Fade

The evolution of the LTO-based battery capacity during cycle aging under TC3 conditions is presented in Fig. 3. Initially, the battery capacity has shown an increase, before starting to decline; a similar behavior was reported in [15] for an NMC-based Li-ion battery cell. One cause for this behavior can be related to an increased electrode active surface area, which resulted from electrochemical milling [15].

In order to evaluate the capacity fade caused by cycle ageing of the LTO-based battery cells at the considered conditions (see Table II) and to analyze its dependence on the stress factors, the measured capacity during the RPTs was related to the capacity measured at beginning of life (BOL), according to (1).

$$Capacity\ [\%] = Capacity_{actual} / Capacity_{BOL} \cdot 100\ \% \qquad (1)$$

Where $Capacity_{actual}$ [Ah] represents the battery actual capacity measured during the RPTs and $Capacity_{BOL}$ [Ah] represents the battery capacity measured at the cells' BOL.

Fig. 4 presents the obtained capacity fade behavior of the two LTO-based battery cells, which were aged according to the TC3 conditions. As it is shown, a very similar degradation behavior were obtained for both battery cells. Thus, for the upcoming analyzes, the average of the capacity fade, which had been obtained for the two cells tested in each TC, was considered.

a) Influence of the C-rate: The influence of the C-rate on the capacity fade for the case when the LTO-based battery cells were cycled at 42.5°C is presented in Fig. 5. As one can observe, the capacity fade is accelerated by decreasing the cycling C-rate from 3C to 1C. A similar behavior was observed for the cells cycled at 50°C (see Fig. 6); the LTO-based cells lost 20% of their capacity after approximately 3000 FEC when cycled at 1C, while they were able to withstand more than 4000 FEC when cycled with 2C. Groot et al., have reported in [16], a similar dependence of the capacity fade on the cycling C-rate for a lithium iron phosphate battery.

Furthermore, the same degradation behavior of the battery capacity can be noticed for all the five cycle aging cases presented in Fig. 5 and Fig. 6. The capacity fade evolution can be divided into three regions, as highlighted in Fig. 4. Initially, an increase of the capacity of the LTO battery cells was noticed independently of the considered accelerated aging conditions. After reaching a maximum point, the capacity of the cells started to decreases slowly (region 2), until an inflection point was reached, from where a fast capacity fade behavior is observed (region 3). This inflection point (referred in literature as aging knee) suggests a change in the dominant aging mechanism of the tested LTO battery cells [17].

The results that are shown in Fig. 5 and Fig. 6 also suggest a very long lifetime for the tested LTO-based battery cells. For example, the batteries cycled with 3C at 42.5°C were able to perform more than 8000 FEC before reaching 10% capacity fade. Moreover, by comparing the results obtained for 42.5°C (Fig. 3) and 50°C (Fig. 4), the effect of the temperature on the capacity fade is the one expected; the LTO-based cells were able to perform approximately 1500 more FEC when cycled at 42.5°C than at 50°C when the same C-rate (i.e., 2C) was considered.

b) Influence of the cycle depth: The dependence of the capacity fade on the cycle depth is presented in Fig. 7 for the case when the battery cells were cycled at 42.5°C. In the beginning of the accelerated aging process, the cells cycled considering a 10% cycle depth have degraded faster than the cells cycled considering a 50% cycle depth. Nevertheless, after 3000 FEC, when the cells had reached less than 4% capacity fade, the aforementioned trend has reversed and an acceleration of the capacity fade with increasing the cycle depth is illustrated. This behavior is in good agreement with results presented in the literature for different Li-ion battery chemistries. Furthermore, the effect of the cycle depth on the capacity fade, which was observed for a cycling temperature of 42.5°C, is consistent with the capacity fade behavior observed for a cycling temperature of 50°C, which is presented in Fig. 8.

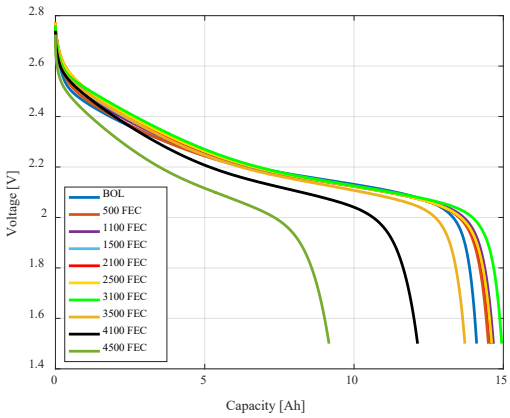

Fig. 3. LTO-based battery capacity evolution during TC3 cycle aging.

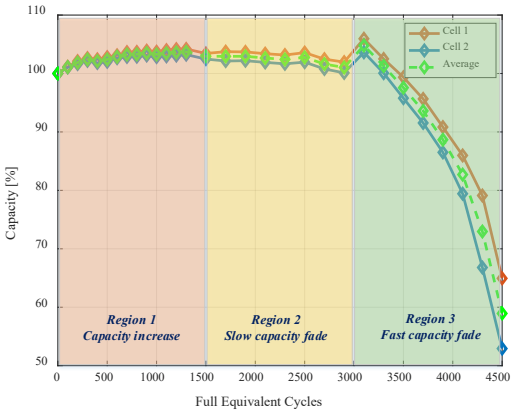

Fig. 4. Capacity fade behavior for two cells aged at similar conditions (used for exemplification – TC3: T = 50°C, 50% cycle depth, 2C charging / discharging).

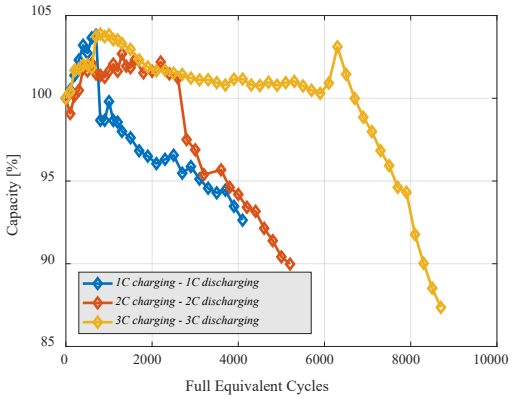

Fig. 5. Capacity fade of LTO-based battery cells cycled at 42.5°C, 50% cycle depth, and different C-rates.

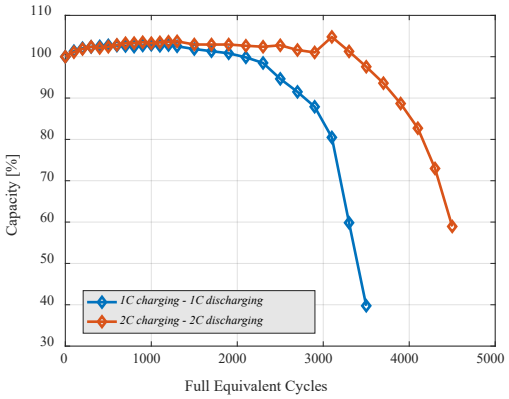

Fig. 6. Capacity fade of LTO-based battery cells cycled at 50 °C, 50% cycle depth, and different C-rates.

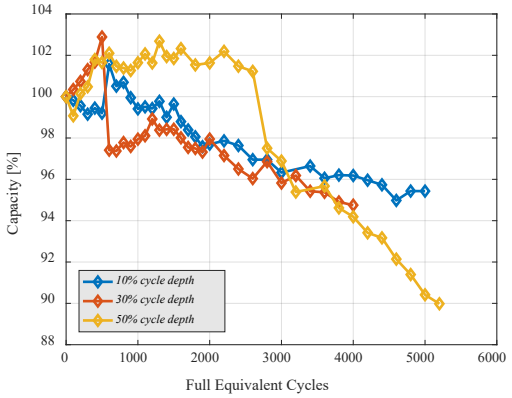

Fig. 7. Capacity fade of LTO-based battery cells cycled at 42.5 °C with 2C-rate and different cycle depths.

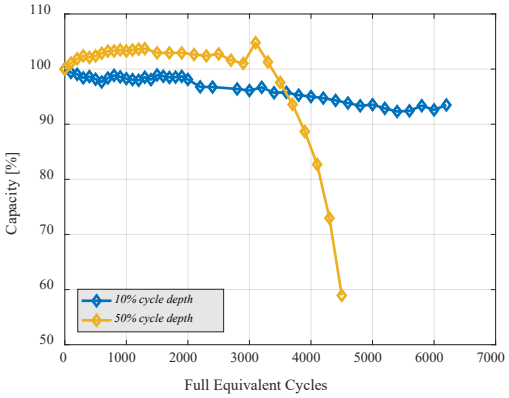

Fig. 8. Capacity fade of LTO-based battery cells cycled at 50 °C with 2C-rate and different cycle depths.

B. *Internal Resistance Increase*

The increase of the internal resistance, $IR_{increase}$, of the LTO-based battery cells, which was caused by aging at the conditions summarized in Table II, was obtained using (2).

$$IR_{increase}\,[\%] = IR_{actual} / IR_{BOL} \cdot 100\,\% \qquad (2)$$

Where IR_{actual} [Ω] represents the battery internal resistance measured during the RPTs and IR_{BOL} [Ω] represents the battery internal resistance measured at the cells' BOL.

During the RPTs, the internal resistance was measured at different SOCs and with different currents. However, for evaluating the increase of the internal resistance due to cycle aging, the internal resistance measured for a 1C-rate (i.e., 13 A) discharging current pulse was considered. Furthermore, by analyzing the internal resistance increase, when the resistance was measured at different SOCs, very similar degradation trends were observed, as it is illustrated in Fig. 9. The increase of the internal resistance varied between the considered SOCs with less than 10%, independently on the number of FECs considered. Consequently, for further analyzing the obtained results, the internal resistance increase obtained at 60% SOC was considered.

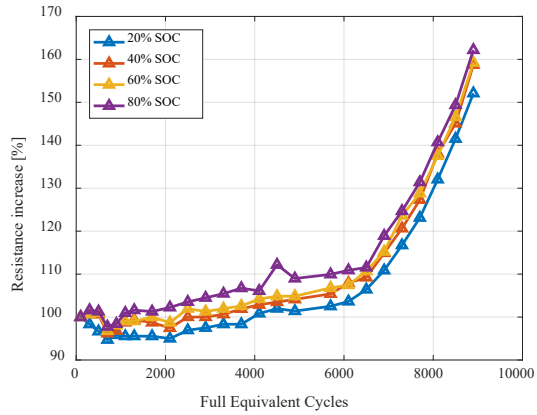

Fig. 9. Internal resistance increase at different SOC levels (LTO-based battery cells aged under TC8 conditions).

a) Influence of the C-rate: The effect of the C-rate on the internal resistance increase for the LTO-based battery cells cycled at 42.5°C and 50°C are presented in Fig. 10 and Fig. 11, respectively. For both cases, higher cycling C-rates have resulted in a faster increase of the cells' internal resistance; for example, for the LTO-based battery cells cycled at 42.5°C and a cycle depth of 50%, 15% internal resistance increase was achieved after 4000 FEC, 5500 FEC, and 7000 FEC when cycled with 1C, 2C, and 3C, respectively.

b) Influence of the cycle depth: The dependence of the internal resistance increase on the cycle depth obtained during cycling at 42.5°C and 50°C is shown in Fig. 12 and Fig. 13, respectively. As it can be observed in Fig. 12, a longer lifetime is expected if the LTO-based battery cell is cycled with larger cycle depths. Initially, the same degradation trend was observed for the cells cycled at 50°C as presented in Fig. 13; however, after the internal resistance has increased by 50%, the previously mentioned trend is reversed and cycling the cells with larger cycle depths resulted in a faster internal resistance increase.

By analyzing the results presented in Fig. 10 – Fig. 13, one can conclude that the increase of the internal resistance of the LTO-based battery cells is rather limited for the considered cycle aging conditions. For the cells cycled at 42.5°C, in only one case the internal resistance has increased by more than 20% even though up to 7000 FEC were performed. A 200% internal resistance increase, which is sometimes referred as the battery end of life criterion from resistance perspective [18], was reached only by the cells cycled at 50°C and 50% cycle depth (Fig. 11); however, this has happened only after more than 3000 FEC, time in which the capacity of the same LTO-based battery cells has already faded with more than 20% (see Fig. 6).

IV. Lifetime Modeling

The influence of the cycle depth on the capacity fade behavior, when the LTO-based battery cells were cycled with 2C-rate at 42.5°C, is presented in Fig. 7. In order to generalize this behavior, the capacity fade caused by cycling at different cycles depths were fitted using the power function (3), as presented in Fig. 15. Even though the power function fits accurately the measured capacity fade, it has to be highlighted that capacity fade values between 5% and 10% were used, to estimate a degradation behavior up to 20% capacity fade.

$$C_{fade}\,[\%] = x \cdot FEC^{\,y} \tag{3}$$

where x represents coefficient and y represents the exponent of the power law function; both x and y are dependent on the cycle depth.

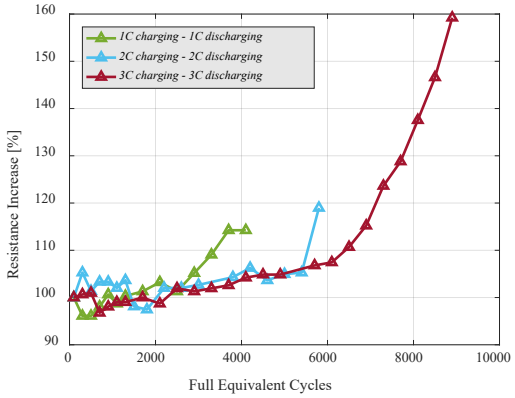

Fig. 10. Internal resistance increase of LTO-based battery cells cycled at 42.5°C, 50% cycle depth, and different C-rates.

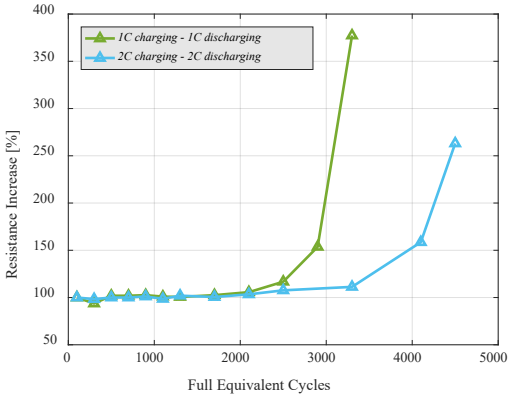

Fig. 11. Internal resistance increase of LTO-based battery cells cycled at 50 °C, 50% cycle depth, and different C-rates.

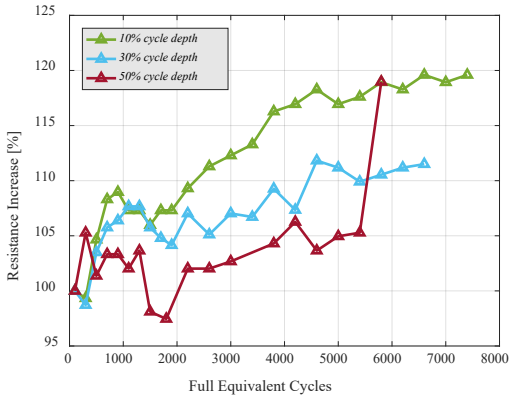

Fig. 12. Internal resistance increase of LTO-based battery cells cycled at 42.5 °C with 2C-rate and different cycle depths.

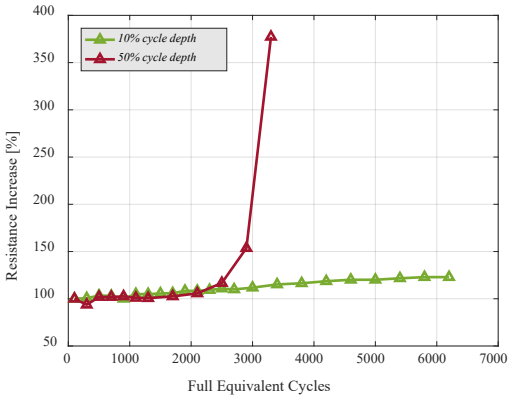

Fig. 13. Internal resistance increase of LTO-based battery cells cycled at 50 °C with 2C-rate and different cycle depths.

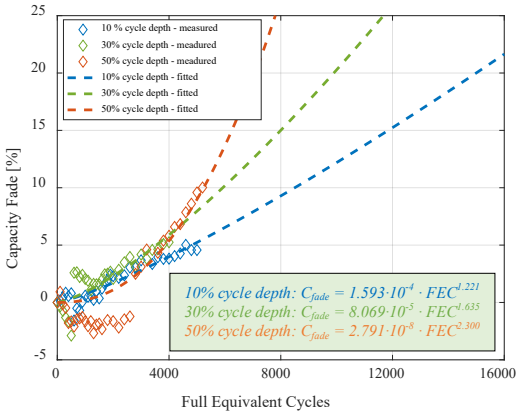

Fig. 14. Estimation of the measured capacity fade using a power law function; cycle aging at 42.5ºC and 2C-charging / 2C-rate discharging for different cycle depths.

Based on the obtained curve fitting results, illustrated in Fig. 15, a general lifetime model, which is able to predict the capacity fade of the LTO-based battery cells when cycled during both charging and discharging with 2C-rate at 42.5°C was derived:

$$C_{fade}\,[\%] = (7.07 \cdot 10^{-4} \cdot e^{-0.149 \cdot cd}) \cdot FEC^{0.443 \cdot cd^{0.4109}} \quad (4)$$

According to the lifetime model (4), the LTO-based battery cells are able to withstand approximately 5180 FEC, before reaching 20% capacity fade when cycling with 100% cycle depth is considered. Furthermore, based on the data sheet of these specific LTO-based battery cells, they are able to perform at least 4 000 FEC and 16 000 FEC when cycled with 2C during both charging and discharging at 55°C and 25°C, respectively. Consequently, these three data points were curve fitted in order to develop a lifetime model, which is able to predict the number of 100% cycle depth FECs that the LTO-based battery cells can perform at different temperature, before they reach an EOL criterion of 20% capacity fade. As shown in Fig. 16, the number of FECs depends exponentially on the cycling temperature T, according to (5).

$$No.\ of\ FECs = 6.328 \cdot 10^{4} \cdot e^{-0.5534 \cdot T} \quad (5)$$

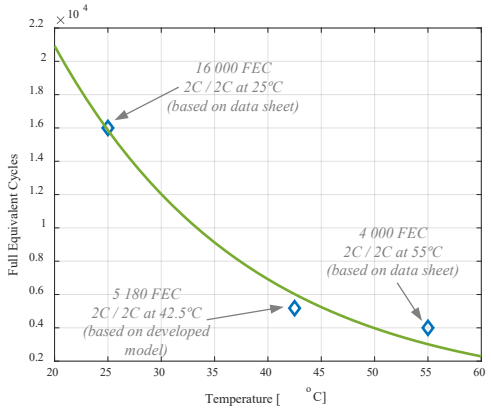

Fig. 15. Variation with cycling temperature of the number of FECs that the LTO-based battery cell can withstand until 20% capacity fade is reached; for the fitting process, a coefficient of deteremination R^2 equal to 0.9806 was obtained.

V. Conclusions

In this paper, results obtained from extended accelerated cycling aging tests of high-power LTO-based Li-ion battery cells were presented. The degradation behavior of battery cells was assessed from both capacity fade and internal resistance increase perspectives. The obtained aging results have shown an unexpected dependence of the battery capacity fade on the cycling C-rate; namely, the capacity fade has been accelerated by decreasing the cycling C-rate. Nevertheless, these results are consistent with the results obtained for the internal resistance, which show also a faster degradation, when the cycling C-rate is decreased gradually from 3C to 1C.

Even though tested at high temperatures, above 40°C, the tested battery cells have shown a very slow degradation, being able to withstand up to 8000 FEC without losing more than 10% of their capacity and an increase of 50% in the internal resistance, which are well below the EOL criterions considered in nowadays applications.

Furthermore, based on the obtained accelerated aging results and information from the battery cell datasheet, a lifetime model was developed. This model is able to estimate the number of FECs that the considered LTO-based battery cells can perform for a wide range of temperatures, before a 20% capacity fade EOL criterion is reached.

Acknowledgment

This work has been part of the “ALPBES – Advanced Lifetime Predictions of Battery Energy Storage” research project, which was financially supported by The Danish Council for Strategic Research.

References

[1] C. Pillot, “Lithium ion battery raw material Supply & demand 2016-2025,” AABC Europe, Mainz, Germany, January 2017.

[2] A. Farmann, W. Waag, and D.U. Sauer, “Application-specific electrical characterization of high power batteries with lithium Titanate anodes for electric vehicles,” Energy, vol. 112, pp. 294-306, 2016.

[3] P. C. Kjær and R. Lærke, "Experience with primary reserve supplied from energy storage system," *17th European Conference on Power Electronics and Applications (EPE'15 ECCE-Europe)*, Geneva, 2015.

[4] L. Gaillac *et al.*, "Tehachapi Wind Energy Storage Project: Description of operational uses, system components and testing plans," *PES T&D 2012*, Orlando, FL, 2012, pp. 1-6.

[5] B. Scrosati, J. Garche, W. Tillmetz, “Advances in battery technology for electric vehicles,” Woodhead Publishing Series, ISBN: 978-1-78242-377-5, 2015.

[6] A.-I. Stan et al., “Lithium Ion Battery Chemistries from Renewable Energy Storage to Automotive and Back-up Power Applications – An Overview,” 2014 International Conference on Optimization of Electrical and Electronic Equipment (OPTIM), pp. 713-720, 2014.

[7] P. Krtil and D. Fattakhova, “Li Insetrion into Li-Ti-O Spinels: Voltametric and Electrochemical Impedance Spectrosocpy Study,” Journal of The Electrochemical Society, vol. 148, pp. A1045-A1050, 2001.

[8] B. Scrosati and J. Garche, “Lithium batteries: Status, prospects and future,” Journal of Power Sources, vol. 195, pp. 2419-2430, 2010.

[9] A. Y. Shenouda and K. R. Murali, “Electrochemical properties of doped lithium titanate compunds and their performance in lithium rechargeable batteries,” Journal of Power Sources, vol. 176, no. 1, pp. 332-339, 2008.

[10] Y. Yang et al., “Lithium Titanate Tailored by Cathodically Induced Graphene for Ultrfast Lithium Ion Battery,” Advanced Functional Materials, vol. 24, no. 27, pp. 4349 – 4356, 2014.

[11] A. I. Stroe, et al., "Performance model for high-power lithium titanate oxide batteries based on extended characterization tests," 2015 IEEE Energy Conversion Congress and Exposition *(ECCE)*, Montreal, 2015.

[12] D.-I. Stroe, M. Swierczynski, A.-I. Stan, R. Teodorescu, S. J. Andreasen, "Accelerated lifetime testing methodology for lifetime estimation of lithium-ion batteries used in augmented wind power plants," IEEE Transactions on Industry Applications, vol. 50, no. 6, pp. 4006-4017, Nov.-Dec. 2014.

[13] J. Schmalstieg, S. Käbitz, M. Ecker and D. U. Sauer, "From accelerated aging tests to a lifetime prediction model: Analyzing lithium-ion batteries," *2013 World Electric Vehicle Symposium and Exhibition (EVS27)*, Barcelona, 2013, pp. 1-12.

[14] A.-I. Stroe, "Analysis aof Performance and Degradation for Lithium Titanate Oxide Batteries," PhD dissertation, Aalborg University, 2018.

[15] J. de Hoog et al., "Combined cycling and calendar capacity fade modeling of a Nickel-Managnese-Cobalt Oxide Cell with real-life profile validation," Applied Energy, vol. 200, pp. 47-61, 2017.

[16] J. Groot et al., "On the complex ageing characteristics of high-power LiFePO4/graphite battery cells cycled with high charge and discharge currents," Journal of Power Sources, vol. 286, pp.475-487, 2015.

[17] E. Martinez-Laserna *et al*., "Evaluation of lithium-ion battery second life performance and degradation," *2016 IEEE Energy Conversion Congress and Exposition (ECCE)*, Milwaukee, WI, 2016, pp. 1-7.

[18] M. Ecker et al., "Development of a lifetime prediction model for lithium-ion batteries based on extended accelerated aging test data," Journal of Power Sources, vol. 2015, pp. 248-257, 2012.